

Cosmological Constraints on $f(R)$ Acceleration Models

Yong-Seon Song, Hiranya Peiris,* and Wayne Hu†

*Kavli Institute for Cosmological Physics,
Department of Astronomy & Astrophysics,
and Enrico Fermi Institute,
University of Chicago, Chicago IL 60637*

(Dated: October 24, 2018)

Models which accelerate the expansion of the universe through the addition of a function of the Ricci scalar $f(R)$ leave a characteristic signature in the large-scale structure of the universe at the Compton wavelength scale of the extra scalar degree of freedom. We search for such a signature in current cosmological data sets: the WMAP cosmic microwave background (CMB) power spectrum, SNLS supernovae distance measures, the SDSS luminous red galaxy power spectrum, and galaxy-CMB angular correlations. Due to theoretical uncertainties in the nonlinear evolution of $f(R)$ models, the galaxy power spectrum conservatively yields only weak constraints on the models despite the strong predicted signature in the linear matter power spectrum. Currently the tightest constraints involve the modification to the integrated Sachs-Wolfe effect from growth of gravitational potentials during the acceleration epoch. This effect is manifest for large Compton wavelengths in enhanced low multipole power in the CMB and anti-correlation between the CMB and tracers of the potential. They place a bound on the Compton wavelength of the field be less than of order the Hubble scale.

PACS numbers:

I. INTRODUCTION

Cosmic acceleration can arise either from an unknown component of dark energy with negative pressure or a modification to gravity that only appears at cosmological scales and densities. Additional terms in the Einstein-Hilbert action that are non-linear functions $f(R)$ of the Ricci scalar R have long been known to cause acceleration [1, 2, 3, 4] and have been the subject of much recent interest [5, 6, 7, 8, 9, 10, 11, 12, 13, 14, 15, 16, 17, 18, 19, 20, 21, 22, 23, 24, 25, 26, 27, 28, 29, 30].

The main challenge for $f(R)$ models as a complete description of gravity lies with the extremely tight constraints on such modifications placed by solar system and local tests of general relativity. Chiba [31] showed that the fundamental problem is that $f(R)$ models generically introduce a light scalar degree of freedom with a long Compton wavelength at cosmological densities [32, 33]. This problem can be mitigated by the so-called chameleon mechanism [34, 35], where the local Compton wavelength can decrease in high density environments [36, 37]. The cosmological Compton wavelength can then be a scale of cosmological interest. Nevertheless, it must typically be less than a few tens of Mpc if the Galactic gravitational potential is not substantially deeper than implied by local rotation curve measurements [38].

In this *Paper*, we take the perspective that $f(R)$ models are effective theories that are valid at cosmological densities and scales and are not necessarily predictive at

the high densities and small scales of local tests. Hence we explore models with Compton wavelengths out to the horizon size and seek to constrain them from cosmological observables alone. At the very least, this exploration yields a cosmological test of general relativity that is independent of local constraints.

Although $f(R)$ models can change the expansion history during the acceleration epoch, there in principle always exists a dark energy model that provides the same history. The unique and strongest signatures of $f(R)$ modifications are on cosmological structure formation [25] and can impact observables down to Compton wavelengths of a few Mpc [38]. We consider constraints arising from the CMB angular power spectrum measured by WMAP [39], the linear matter power spectrum inferred from the Sloan Digital Sky Survey (SDSS) luminous red galaxy (LRG) sample [40], the distance measures by the Supernovae Legacy Survey (SNLS) [41], and the cross-correlation between the CMB and large scale structure as measured by WMAP and a range of galaxy and quasar surveys [42, 43, 44, 45, 46].

The outline of the paper is as follows. In §II, we review the $f(R)$ model and discuss our calculation and analysis methods. In §III we present the results of joint cosmological constraints on these models. We discuss these results in §IV.

II. $f(R)$ METHODOLOGY

A. Model

In $f(R)$ models of gravity, the Einstein-Hilbert action is supplemented by a term that is non-linear in the Ricci

*Hubble Fellow

†Electronic address: ysong@kicp.uchicago.edu

scalar R

$$S = \int d^4x \sqrt{-g} \left[\frac{R + f(R)}{16\pi G} + \mathcal{L}_m \right], \quad (1)$$

where \mathcal{L}_m is the matter Lagrangian. The modified Einstein and Friedmann equations result from varying the action with respect to the metric. Given the freedom to choose a functional form for $f(R)$, any desired expansion history can be replicated [6, 20, 25, 47, 48, 49]. In particular, one can choose the Λ CDM expansion history which is known to satisfy distance constraints from high redshift supernovae, baryon acoustic oscillations and the CMB.

Even given the degeneracy with dark energy in the expansion history, $f(R)$ models have distinguishable effects on the formation of structure. The promotion of the Ricci scalar to a dynamical degree of freedom modifies the force law between particles. This modified force is mediated by a new scalar degree of freedom $f_R \equiv df/dR$, which has a squared Compton wavelength proportional to $f_{RR} \equiv d^2f/dR^2$. Below the Compton wavelength scale gravity becomes a scalar-tensor theory, leading to an enhancement in the growth of cosmological density perturbations and a corresponding suppression in the decay of gravitational potentials.

For cosmological tests, it is convenient to express the squared Compton wavelength in the background in units of the Hubble length squared [25, 50]

$$B \equiv \frac{f_{RR}}{1 + f_R} \frac{dR}{d \ln a} \left(\frac{d \ln H}{d \ln a} \right)^{-1}, \quad (2)$$

where a is the scale factor and the Ricci scalar is evaluated at the background density. We will specialize our consideration to $f(R)$ models that exactly reproduce the Λ CDM expansion history to test whether the unique signatures of $f(R)$ gravity are seen in current cosmological data sets.

Under this assumption, the additional degree of freedom in $f(R)$ gravity is parameterized by the value of B today, $B_0 \equiv B(z=0)$. Stability requires the mass squared of the scalar to be positive (*i.e.* a prior of $B_0 \geq 0$) [25, 26]. Note that in the limit that $B_0 \rightarrow 0$, the phenomenology of Λ CDM is recovered in structure formation tests as well as expansion history tests. More generally, the control parameter is the average Compton wavelength through the acceleration epoch when gravity is modified.

B. Power Spectra Calculation

The fundamental observables of our $f(R)$ model are the same as in Λ CDM. These include the redshift-distance relation, the CMB angular power spectrum C_ℓ , galaxy power spectra $P_g(k)$, and the angular correlation between galaxies and the CMB $w(\theta)$. Cosmic shear, dark matter halo profiles and masses from weak lensing as

well as the cluster abundance are also potential observables but their utilization requires cosmological simulations that are beyond the scope of this work.

We modified the Boltzmann code CAMB [51] to calculate these observables in $f(R)$ gravity. In the CAMB code, the density perturbations are computed in the synchronous gauge. We evolve the usual Boltzmann code up to $a \sim 0.01$ when deviations introduced by $f(R)$ are still small. At this epoch, we transform the matter perturbations from synchronous gauge to gauge invariant variables, and feed them as initial conditions to the linear perturbation equations for the density fluctuation and CMB sources (see [25] Eqs. 28-35). Once the initial conditions are specified, the power spectrum observables are computed from a separate $f(R)$ routine that bypasses the usual CAMB code without significantly increasing the computational time.

As we shall discuss, the main modification made by our $f(R)$ models on the CMB is a change in the evolution of gravitational potentials during the acceleration epoch. The CMB power spectrum is modified at low multipoles through the so called ‘‘Integrated Sachs-Wolfe’’ (ISW) effect, and the temperature field is correlated with tracers of gravitational potentials such as galaxies. This correlation is strong if the redshift of the galaxies is matched to the epoch at which the gravitational potentials evolve. Following [52], we model the angular correlation between a set of galaxy surveys indexed by i and the CMB, assuming a broad band selection function for the galaxies,

$$n_i(z) = \frac{1.5}{\Gamma[2]} \frac{z^2}{z_i^3} e^{-(z/z_i)^{1.5}}, \quad (3)$$

where the z_i are chosen to match the median redshift in the surveys. While crude, the uncertainties introduced by this choice of selection function are smaller than the difference in model predictions that will be considered. The galaxy bias is assumed to be constant in each redshift bin. We calculate the cross power spectrum between galaxy number density and CMB temperature following [25] (Eqs. 55-60) and transform it to the angular power correlation function $w_i(\theta)$.

C. Likelihood Analysis

We use a Markov Chain Monte Carlo (MCMC) technique [53, 54, 55, 56, 57, 58] to evaluate the likelihood function of model parameters. The MCMC is used to simulate observations from the posterior distribution $\mathcal{P}(\boldsymbol{\theta}|x)$, of a set of parameters $\boldsymbol{\theta}$ given event x , obtained via Bayes’ Theorem,

$$\mathcal{P}(\boldsymbol{\theta}|x) = \frac{\mathcal{P}(x|\boldsymbol{\theta})\mathcal{P}(\boldsymbol{\theta})}{\int \mathcal{P}(x|\boldsymbol{\theta})\mathcal{P}(\boldsymbol{\theta})d\boldsymbol{\theta}}, \quad (4)$$

where $\mathcal{P}(x|\boldsymbol{\theta})$ is the likelihood of event x given the model parameters $\boldsymbol{\theta}$ and $\mathcal{P}(\boldsymbol{\theta})$ is the prior probability density. The MCMC generates random draws (*i.e.* simulations)

from the posterior distribution that are a “fair” sample of the likelihood surface. From this sample, we can estimate all of the quantities of interest about the posterior distribution (mean, variance, confidence levels). A properly derived and implemented MCMC draws from the joint posterior density $\mathcal{P}(\boldsymbol{\theta}|x)$ once it has converged to the stationary distribution. We use 16 chains and a conservative Gelman-Rubin convergence criterion [59] to determine when the chains have converged to the stationary distribution.

For our application, $\boldsymbol{\theta}$ denotes a set of cosmological parameters. We then use a modified version of the CosmoMC code [56] to determine constraints placed on this parameter space by WMAP, SDSS LRG galaxy power spectrum, and supernova distance measures. For the LRG data, we only use the first 14 k -bins in our fits reflecting a conservative cut for linearity $k < 0.1h/\text{Mpc}$. For the supernovae constraint, we take the Supernovae Legacy Survey data set and its analysis remains unaffected by our $f(R)$ modification. Likewise, its impact is mainly to help determine expansion history parameters. In our analysis, we take the parameter set $\{\omega_b \equiv \Omega_b h^2, \omega_m \equiv \Omega_m h^2, \theta_A, \ln(10^{10} A_s), n_s, \tau, B_0, b, Q_{\text{nl}}\}$, where θ_A is the angular size of the acoustic horizon, and A_s is the power in the primordial curvature perturbation at $k = 0.05 \text{ Mpc}^{-1}$. The universe is assumed to be to be spatially flat. Recall also that we fix the expansion history to be the same as a ΛCDM model. Hence θ_A is also a proxy for the Hubble constant $H_0 \equiv 100h \text{ km/s/Mpc}$ or Ω_m .

The last two parameters in the set are the linear galaxy bias b and non-linearity parameter Q_{nl} required for the interpretation of the galaxy power spectrum $P_g(k)$ of SDSS LRGs [40] (see also §III B), defined as

$$P_g(k) = P_L(k) b^2 \frac{1 + Q_{\text{nl}} k^2}{1 + 1.4k}. \quad (5)$$

The linear bias factor b is defined with respect to the linear matter power spectrum $P_L(k)$ at $z = 0.35$, the effective redshift of the LRG galaxies. Since $f(R)$ models predict a scale dependent growth rate that changes the shape of the power spectrum as a function of redshift, we do not define the bias as relative to the power spectrum at $z = 0$ (*cf.* [40]). The second factor on the right hand side accounts for the non-linear evolution of the matter power spectrum shape and the scale-dependent bias of the galaxies relative to dark matter. We assume that this *ansatz* continues to be a valid approximation for $f(R)$ theories. We do not marginalize analytically over the b and Q_{nl} parameters as is done normally in the CosmoMC code; instead the parameters are marginalized numerically as independent nuisance parameters in the MCMC analysis.

For all of our parameters except for B_0 , we employ flat linear priors in the stated parameters. For B_0 , we supplement the flat prior with the stability condition that $B_0 \geq 0$.

Finally, these constraints are projected onto the space

of the galaxy-ISW angular correlation function for comparison with the data. We do not attempt here to include the correlation function data in the likelihood. That would require a joint re-analysis of the various data sets to capture the covariance between the measurements. It would also require an assessment of systematic errors in the correlation due to uncertainties in the selection functions and other effects. Instead we compare predictions with the individual measurements and their errors as quoted in the literature.

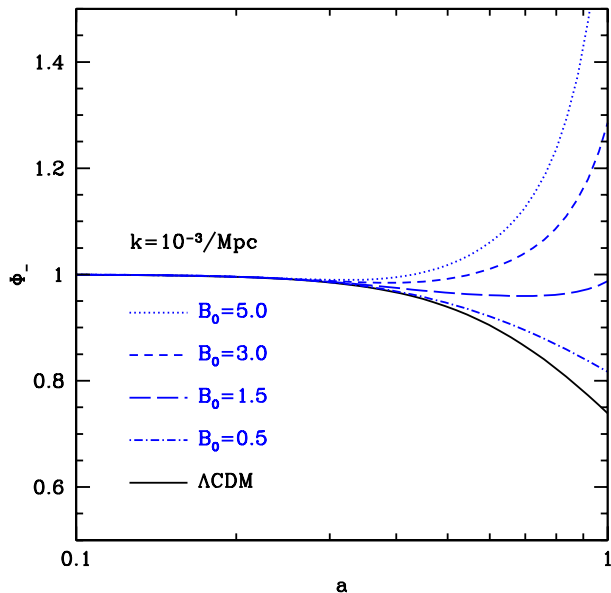


FIG. 1: Time evolution of the effective gravitational potential $\Phi_- = (\Phi - \Psi)/2$ for $k = 10^{-3}/\text{Mpc}$ near the peak contribution to the ISW effect at low multipoles. As the Compton wavelength parameter B_0 increases, the decay of the gravitational potential in ΛCDM decreases and eventually turns to growth. This reversal changes the sign of the ISW effect in overdense regions traced by galaxies.

III. COSMOLOGICAL CONSTRAINTS

A. CMB

In $f(R)$ models that follow the ΛCDM expansion history considered here, none of the CMB phenomenology at recombination is affected by the modification to gravity. The Compton wavelength parameter B is driven rapidly to zero at high density and curvature. Hence all of the successes of ΛCDM in explaining the acoustic peaks carries over to these $f(R)$ models.

The impact of $f(R)$ gravity on the CMB comes exclusively through the so-called Integrated Sachs-Wolfe (ISW) effect at the lowest multipole moments. The ISW effect arises from an imbalance between the blueshift a CMB photon suffers while falling into a gravitational

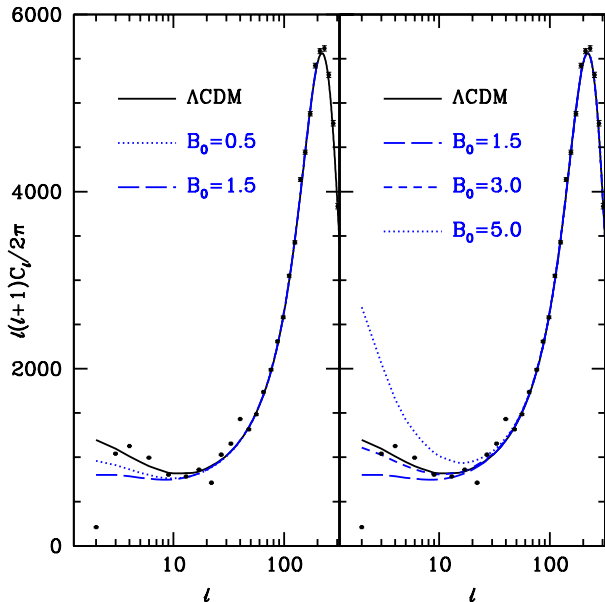


FIG. 2: CMB angular power spectrum C_ℓ for $f(R)$ models with the Compton wavelength parameter $B_0 = 0$ (Λ CDM), 0.5, 1.5, 3.0, 5.0. As B_0 increases, the ISW contributions to the low multipoles decrease, change sign, and then increase. WMAP3 data with noise error bars are overlotted and rule out $B_0 \geq 4.3$ (95% CL).

potential well and the redshift while climbing out if the gravitational potential evolves during transit. With a cosmological constant, gravitational potentials decay during the acceleration epoch. For $f(R)$ models, the enhancement of the growth rate below the Compton scale can change the decay into growth (see Fig. 1). This reversal changes the sign of the ISW effect. CMB photons then become colder along directions associated with overdense regions.

Fig. 2 illustrates the impact of this effect on the CMB power spectrum. As the Compton wavelength approaches the Gpc ($k \sim 10^{-3} \text{ Mpc}^{-1}$) scales associated with the low multipoles of the ISW effect, the reduction in the decay of the potential also suppresses the ISW effect. Near $B_0 \approx 1.5$ the ISW effect is almost entirely absent at the quadrupole. Reduction in the amplitude of the quadrupole is in fact weakly favored by the data but the large cosmic variance of the low multipoles prevents this from being a significant improvement. Moreover, the elimination of the ISW effect at higher multipoles where the observed power is higher counteracts this improvement. For $B_0 \gtrsim 1.5$ the Compton wavelength exceeds the scales of interest and potential decay turns to potential growth. By $B_0 \sim 3$ the ISW effect has an equal amplitude to that of Λ CDM. For $B_0 \gtrsim 5$, it is too large to accommodate the WMAP data. These features drive the overall joint constraint on B_0 shown in Fig. 3. The WMAP data also serve to fix the parameters that control the high redshift universe. In particular, it constrains the

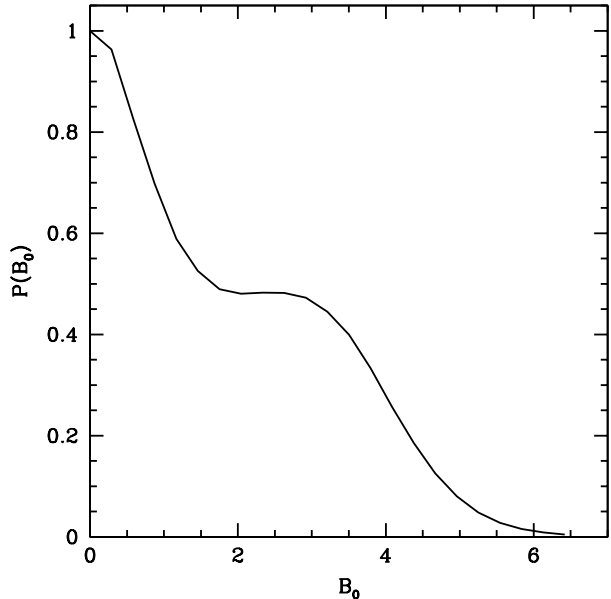


FIG. 3: Posterior probability distribution for the Compton wavelength parameter B_0 inferred from the joint likelihood analysis of WMAP CMB angular power spectrum, SDSS LRG galaxy power spectrum, and SNLS supernovae data. The upper limit on B_0 from the joint constraint is driven by the CMB data, specifically the ISW effect.

initial amplitude of power on scales that are observed in galaxy surveys such as the SDSS LRG survey.

B. Galaxy Power Spectrum

The time-dependent Compton wavelength of $f(R)$ models induces a more dramatic effect in the matter power spectrum during the acceleration epoch. In fact, average Compton wavelengths down to a few Mpc are potentially observable in the linear power spectrum. Under this scale, the enhanced growth rate leads to excess power relative to the same initial power spectrum determined by the WMAP data. Unfortunately the overall change in power is degenerate with the unknown galaxy bias. However if the Compton wavelength appears between the few to 100 Mpc scale the distortion of the shape of the power spectrum is potentially distinguishable in current surveys. In our parameterization this occurs for $B_0 \sim 10^{-5} - 10^{-2}$.

The SDSS LRG data set in fact favor enhanced power over the *linear* Λ CDM power spectrum. In Fig. 4, we compare a linear Λ CDM power spectrum ($\omega_b = 0.025, \omega_m = 0.128, H_0 = 73, 10^{10} A_s = 21.2, n_s = 0.95, \tau = 0.09, B_0 = 0, b = 2.2$) and a linear $f(R)$ power spectrum with the same parameters and $B_0 = 4 \times 10^{-4}$. The $f(R)$ model is in fact a better fit to the shape of the power spectrum, with $\Delta\chi_{\text{eff}}^2 = 2\Delta \ln L \approx 11.5$ for this specific choice of bias.

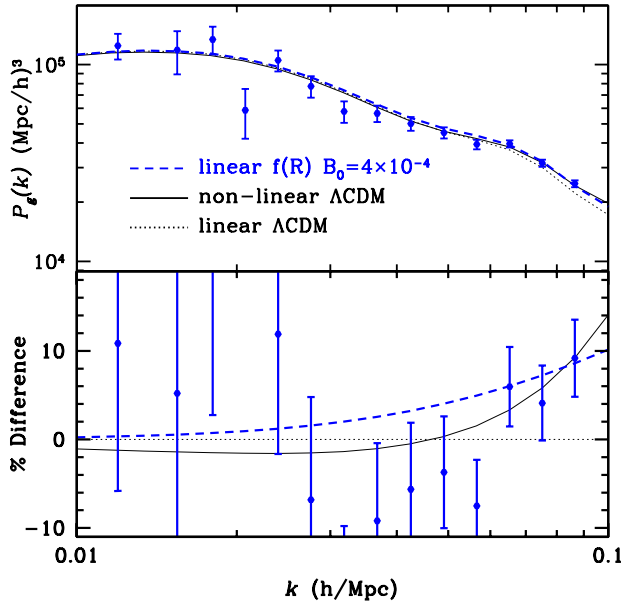


FIG. 4: SDSS LRG galaxy power spectrum data compared with a linear Λ CDM power spectrum (see text), a linear $f(R)$ model with $B_0 = 4 \times 10^{-4}$ and the best fit nonlinear Λ CDM power spectrum. While the data are better fit by $f(R)$ with *linear* power spectra, nonlinearities make Λ CDM a better fit to the data and open up a degeneracy between $f(R)$ modifications parameterized by B_0 and the non-linearity parameter Q_{nl} .

However in the Λ CDM model, we expect LRG galaxy clustering to be nonlinear in exactly the region where these changes of shape occur. In fact a non-linearity parameter of $Q_{nl} = 30$, which represents a reasonable amount of non-linearity, produces an excellent fit to the data (see Fig. 4). Hence, $f(R)$ enhancements of small scale power are degenerate with non-linear effects in Λ CDM and open up a corresponding degeneracy between Q_{nl} and B_0 (see Fig. 5). The non-linear modification also introduces a small suppression of power at intermediate k for any value of Q_{nl} which also marginally improves the fit.

Furthermore if $B_0 \gtrsim 10^{-2}$ the Compton scale exceeds the largest scales in the survey at $k \sim 10^{-2} h/\text{Mpc}$. The enhancement of small scale power, while pronounced, becomes degenerate with the galaxy bias b . With the primordial amplitude fixed by WMAP, the bias must decrease as B_0 increases, leading to an anti-correlation between the two parameters (see Fig. 6).

Even order unity B_0 is allowed after marginalization. The LRG data do weakly disfavor even larger B_0 but the overall constraint is dominated by the CMB data (see Fig. 3 and compare $B_0 = 3$ relative to $B_0 = 0$, where the CMB spectra are nearly identical).

It is the marginalization over the non-linear parameter Q_{nl} and bias which substantially degrades the ability of the LRG data to constrain $f(R)$ models. This is a theoretical and not an observational limitation. As

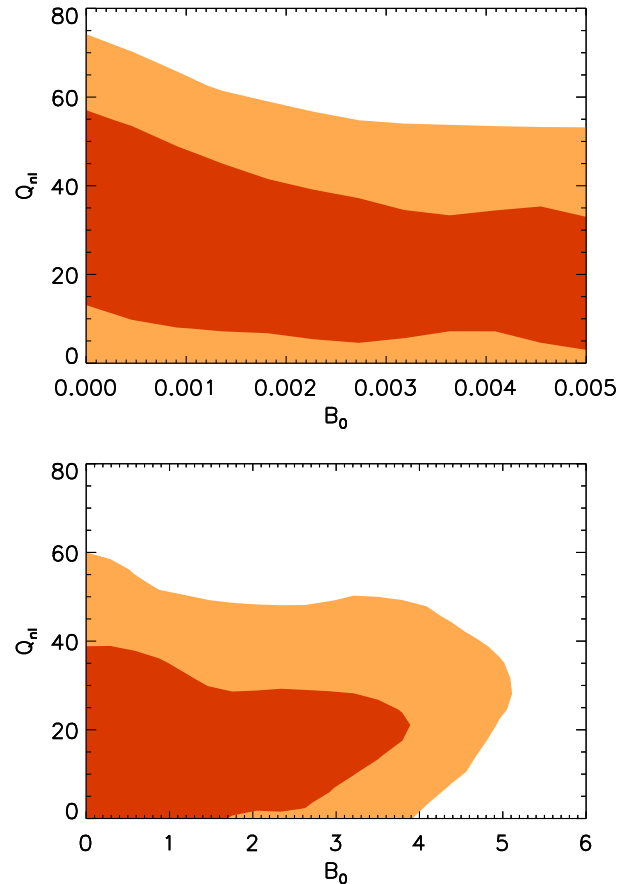


FIG. 5: The 2D joint 68% CL (dark) and 95% CL (light) constraints on the Compton wavelength parameter B_0 and non-linearity parameter Q_{nl} inferred from the joint likelihood analysis of WMAP CMB angular power spectrum, SDSS LRG galaxy power spectrum, and SNLS supernovae data. The upper panel focuses in on the range $B_0 < 0.005$ in order to highlight the anti-correlation between these two parameters discussed in the text, while the lower panel shows the full joint constraint.

we have seen, even the small value of $B_0 \sim 10^{-4}$ substantially impacts the current data. With cosmological simulations that address the non-linear evolution of the matter power spectrum in $f(R)$ and the association of LRG's with dark matter haloes in the simulation, this uncertainty can be lifted leading to substantially tighter bounds on the Compton wavelength.

C. Galaxy-ISW Correlation

The angular correlation between the CMB temperature field and galaxy number density field induced by the ISW effect places an interesting constraint on $f(R)$ models with averaged Compton wavelengths in the > 100 Mpc regime. As discussed in III A, the ISW effect reverses sign for wavelengths smaller than the average Compton wavelength during acceleration. This rever-

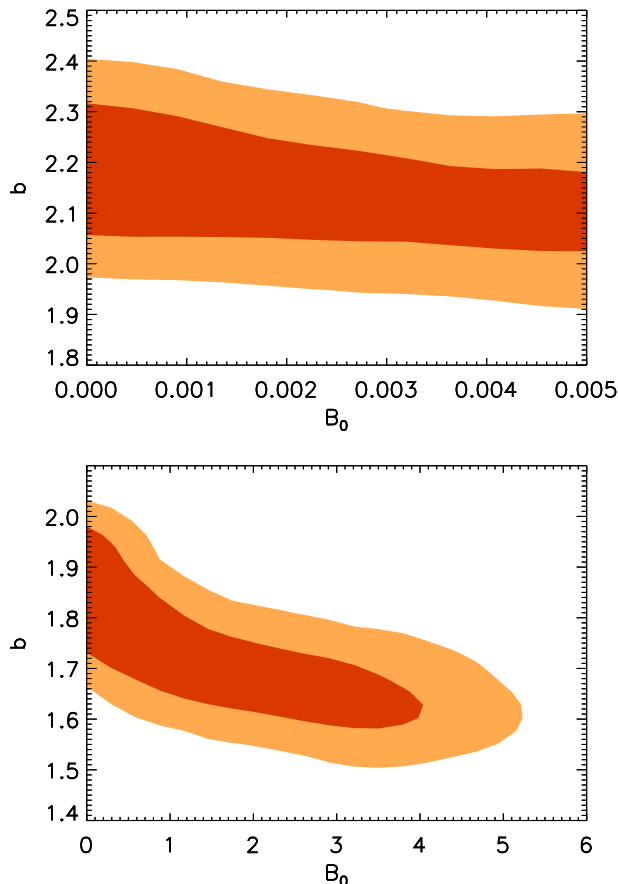


FIG. 6: The 2D joint 68% CL (dark) and 95% CL (light) constraints on the Compton wavelength parameter B_0 and the linear galaxy bias b inferred from the joint likelihood analysis of WMAP CMB angular power spectrum, SDSS LRG galaxy power spectrum, and SNLS supernovae data. The upper panel focuses in on the range $B_0 < 0.005$ in order to highlight the anti-correlation between these two parameters discussed in the text, while the lower panel shows the full joint constraint.

sal of sign causes galaxies to be anti-correlated with the CMB [25]. For sufficiently large $B_0 > 1$, the Compton wavelength subtends a scale larger than the $1 - 10^\circ$ over which the correlation has been measured. In this regime, $f(R)$ models predict that galaxies are anti-correlated with the CMB, in conflict with the data measured by 2MASS, APM, SDSS, NVSS and QSO [42, 43, 44, 45, 46].

Figure 7 shows the angular correlation data at 6° from a compilation in [60] (updated by Gaztanaga, private communication). We compare these data with predictions from models in the chain spanning the 68% and 95% allowed regions given by the WMAP CMB, SDSS LRG power spectrum and supernovae data sets. The lack of anti-correlation in any given data point places an upper bound of $B_0 \lesssim 1$ at the significance level of the detection. This is approximately a factor of 4 improvement in B_0 over the other constraints or a factor of 2 in the Compton wavelength. These individual constraints

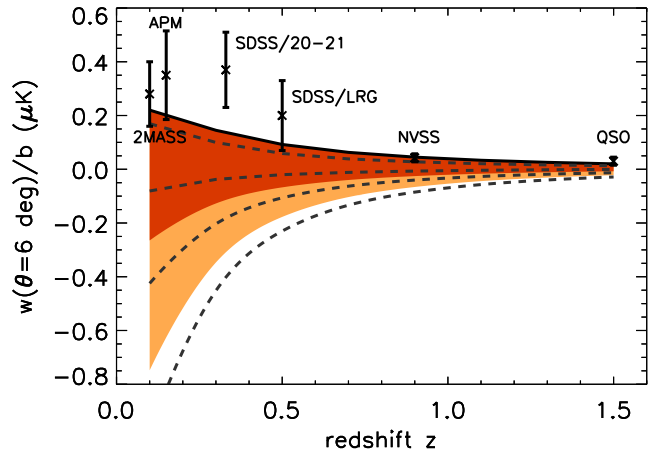


FIG. 7: The galaxy-ISW angular correlation function at 6 degrees is shown as a function of redshift as measured by a variety of surveys (including quasars), with the bias divided out. The constraints on $f(R)$ models given by CMB, SDSS LRG galaxies and supernovae are projected onto this observable, with 68% CL (dark) and 95% CL (light) shaded regions shown. The Λ CDM limit of $B_0 \rightarrow 0$ is shown by a solid line, and the dashed lines (from top to bottom) correspond to $B_0 = \{0.5, 1.5, 3.0, 5.0\}$.

can be improved somewhat by a full joint analysis of the correlation measurements but that lies beyond the scope of this work.

IV. DISCUSSION

We have analyzed current cosmological constraints on $f(R)$ acceleration models from the CMB, SDSS galaxy power spectrum, galaxy-ISW correlations and supernovae. By choosing $f(R)$ models with a Λ CDM expansion history, we have explored whether the unique signatures of the $f(R)$ modification to gravity are seen in current data.

Despite the relatively large impact of $f(R)$ models on the matter power spectrum, the strongest current constraints involve the modification these models induce on the ISW effect in the CMB. The growth of density perturbations is enhanced under the Compton wavelength of the field $f_R = df/dR$ by scalar-tensor modifications to the gravitational force law. This enhancement turns the decay of gravitational potentials during the acceleration epoch in Λ CDM into growth. The joint constraint on the Compton wavelength parameter $B_0 < 4.3$ (95% CL), from the WMAP CMB power spectrum, SDSS galaxy power spectrum and supernovae, is driven by the CMB. This constraint allows Compton wavelengths as large as the current horizon and is a weak bound on $f(R)$ models.

A stronger bound of $B_0 \lesssim 1$ can be inferred from the positive correlation between the CMB and a range of galaxy surveys from $z \sim 0.1 - 1.5$. In Λ CDM this positive

correlation is induced by the ISW effect from a decaying potential. In $f(R)$ models growing potentials convert the positive correlation into anti-correlation in violation of the observations.

The weak impact of the SDSS LRG galaxy power spectrum on our joint constraints is due to a theoretical rather than observational limitation. Intriguingly the *linear* $f(R)$ power spectrum is a marginally better fit to the data than a *linear* Λ CDM one. However the non-linear corrections expected in Λ CDM bring the model back in agreement with the data. N -body simulations have yet to determine the non-linear matter power spectrum and dark matter halo (and hence galaxy) correlations in $f(R)$ models. The likely impact of non-linear evolution is degenerate with the enhancement of small scale linear power seen in $f(R)$ models. When non-linearity of the form expected for Λ CDM is marginalized for $f(R)$ models, the impact of the galaxy power spectrum on joint constraints becomes very weak, and Compton wavelengths out to the horizon length are allowed.

In the future, the window between the horizon length

and a few tens of Mpc can be tested by larger photometric surveys that probe the shape of the power spectrum across the whole range of scales. In principle, Compton wavelengths down to a few Mpc can be tested by galaxy power spectra and cosmic shear from comparison of data with simulations of $f(R)$ models.

Acknowledgments: We thank Ignacy Sawicki for help during the initial phases of this work, Enrique Gaztanaga for the compilation of galaxy-ISW correlation data, and Marilena LoVerde for useful discussions. YS and WH are supported by the U.S. Dept. of Energy contract DE-FG02-90ER-40560. HVP is supported by NASA through Hubble Fellowship grant #HF-01177.01-A awarded by the Space Telescope Science Institute, which is operated by the Association of Universities for Research in Astronomy, Inc., for NASA, under contract NAS 5-26555. WH is additionally supported by the David and Lucile Packard Foundation. This work was carried out at the KICP under NSF PHY-0114422.

-
- [1] A. A. Starobinsky, Phys. Lett. **B91**, 99 (1980).
 - [2] S. M. Carroll, V. Duvvuri, M. Trodden, and M. S. Turner, Phys. Rev. **D70**, 043528 (2004), astro-ph/0306438.
 - [3] S. Capozziello, S. Carloni, and A. Troisi (2003), astro-ph/0303041.
 - [4] S. Nojiri and S. D. Odintsov, Phys. Rev. **D68**, 123512 (2003), hep-th/0307288.
 - [5] N. J. Poplawski, Phys. Rev. **D74**, 084032 (2006), gr-qc/0607124.
 - [6] A. de la Cruz-Dombriz and A. Dobado, Phys. Rev. **D74**, 087501 (2006), gr-qc/0607118.
 - [7] A. W. Brookfield, C. van de Bruck, and L. M. H. Hall, Phys. Rev. **D74**, 064028 (2006), hep-th/0608015.
 - [8] T. P. Sotiriou, Phys. Lett. **B645**, 389 (2007), gr-qc/0611107.
 - [9] T. P. Sotiriou, Class. Quant. Grav. **23**, 5117 (2006), gr-qc/0604028.
 - [10] R. Bean, D. Bernat, L. Pogosian, A. Silvestri, and M. Trodden, Phys. Rev. **D75**, 064020 (2007), astro-ph/0611321.
 - [11] L. Amendola, R. Gannouji, D. Polarski, and S. Tsujikawa, Phys. Rev. **D75**, 083504 (2007), gr-qc/0612180.
 - [12] S. Baghram, M. Farhang, and S. Rahvar, Phys. Rev. **D75**, 044024 (2007), astro-ph/0701013.
 - [13] D. Bazeia, B. Carneiro da Cunha, R. Menezes, and A. Y. Petrov (2007), hep-th/0701106.
 - [14] B. Li and J. D. Barrow, Phys. Rev. **D75**, 084010 (2007), gr-qc/0701111.
 - [15] S. Bludman (2007), astro-ph/0702085.
 - [16] T. Rador (2007), hep-th/0702081.
 - [17] V. Faraoni, Phys. Rev. **D74**, 104017 (2006), astro-ph/0610734.
 - [18] T. Koivisto, Phys. Rev. **D73**, 083517 (2006), astro-ph/0602031.
 - [19] S. Capozziello and R. Garattini, Class. Quant. Grav. **24**, 1627 (2007), gr-qc/0702075.
 - [20] S. Nojiri and S. D. Odintsov, Phys. Rev. **D74**, 086005 (2006), hep-th/0608008.
 - [21] S. Nojiri and S. D. Odintsov (2006), hep-th/0610164.
 - [22] S. Capozziello, S. Nojiri, S. D. Odintsov, and A. Troisi, Phys. Lett. **B639**, 135 (2006), astro-ph/0604431.
 - [23] S. Fay, S. Nesseris, and L. Perivolaropoulos (2007), gr-qc/0703006.
 - [24] L. Amendola and S. Tsujikawa (2007), arXiv:0705.0396 [astro-ph].
 - [25] Y.-S. Song, W. Hu, and I. Sawicki, Phys. Rev. **D75**, 044004 (2007), astro-ph/0610532.
 - [26] I. Sawicki and W. Hu, Phys. Rev. D in press, astro (2007), astro-ph/0702278.
 - [27] S. Tsujikawa (2007), arXiv:0705.1032 [astro-ph].
 - [28] S. A. Appleby and R. A. Battye (2007), arXiv:0705.3199 [astro-ph].
 - [29] C. Charmousis, R. Gregory, and A. Padilla (2007), arXiv:0706.0857 [hep-th].
 - [30] A. De Felice, P. Mukherjee, and Y. Wang (2007), arXiv:0706.1197 [astro-ph].
 - [31] T. Chiba, Phys. Lett. **B575**, 1 (2003), astro-ph/0307338.
 - [32] T. Chiba, T. L. Smith, and A. L. Erickcek (2006), astro-ph/0611867.
 - [33] A. L. Erickcek, T. L. Smith, and M. Kamionkowski, Phys. Rev. **D74**, 121501 (2006), astro-ph/0610483.
 - [34] J. Khoury and A. Weltman, Phys. Rev. **D69**, 044026 (2004), astro-ph/0309411.
 - [35] D. F. Mota and J. D. Barrow, Mon. Not. Roy. Astron. Soc. **349**, 291 (2004), astro-ph/0309273.
 - [36] I. Navarro and K. Van Acoleyen (2006), gr-qc/0611127.
 - [37] T. Faulkner, M. Tegmark, E. F. Bunn, and Y. Mao (2006), astro-ph/0612569.
 - [38] W. Hu and I. Sawicki, Phys. Rev. D submitted (2007), 0705.1158 [astro-ph].
 - [39] D. N. Spergel et al. (2006), astro-ph/0603449.
 - [40] M. Tegmark et al., Phys. Rev. **D74**, 123507 (2006), astro-

- ph/0608632.
- [41] P. Astier et al., *Astron. Astrophys.* **447**, 31 (2006), astro-ph/0510447.
- [42] N. Afshordi, Y.-S. Loh, and M. A. Strauss, *Phys. Rev.* **D69**, 083524 (2004), astro-ph/0308260.
- [43] S. Boughn and R. Crittenden, *Nature* **427**, 45 (2004).
- [44] P. Fosalba and E. Gaztanaga, *Mon. Not. R. Astron. Soc.* **350**, 37 (2004).
- [45] T. Giannantonio et al., *Phys. Rev.* **D74**, 063520 (2006), astro-ph/0607572.
- [46] A. Cabré, E. Gaztañaga, M. Manera, P. Fosalba, and F. Castander, *Mon. Not. R. Astron. Soc.* **372**, L23 (2006), arXiv:astro-ph/0603690.
- [47] T. Multamaki and I. Vilja, *Phys. Rev.* **D73**, 024018 (2006), astro-ph/0506692.
- [48] S. Capozziello, S. Nojiri, S. D. Odintsov, and A. Troisi, *Phys. Lett.* **B639**, 135 (2006), astro-ph/0604431.
- [49] S. Nojiri and S. D. Odintsov (2006), hep-th/0611071.
- [50] P. Zhang, *Phys. Rev.* **D73**, 123504 (2006), astro-ph/0511218.
- [51] A. Lewis, A. Challinor, and A. Lasenby, *Astrophys. J.* **538**, 473 (2000), astro-ph/9911177.
- [52] M. LoVerde, L. Hui, and E. Gaztanaga, *Phys. Rev.* **D75**, 043519 (2007), astro-ph/0611539.
- [53] N. Christensen and R. Meyer (2000), astro-ph/0006401.
- [54] N. Christensen, R. Meyer, L. Knox, and B. Luey, *Class. Quant. Grav.* **18**, 2677 (2001), astro-ph/0103134.
- [55] L. Knox, N. Christensen, and C. Skordis, *Astrophys. J.* **563**, L95 (2001), astro-ph/0109232.
- [56] A. Lewis and S. Bridle, *Phys. Rev. D* **66**, 103511 (2002), astro-ph/0205436.
- [57] A. Kosowsky, M. Milosavljevic, and R. Jimenez, *Phys. Rev.* **D66**, 063007 (2002), astro-ph/0206014.
- [58] L. Verde et al., *Astrophys. J. Suppl.* **148**, 195 (2003), astro-ph/0302218.
- [59] A. Gelman and D. Rubin, *Statistical Science* **7**, 452 (1992).
- [60] E. Gaztanaga, M. Manera, and T. Multamaki, *Mon. Not. Roy. Astron. Soc.* **365**, 171 (2006), astro-ph/0407022.